DOI: 10.1002/cbic.200600176

Differential Protein Assembly on Micropatterned Surfaces with Tailored Molecular and Surface Multivalency

Ramūnas Valiokas,[b] Goran Klenkar,[c] Ali Tinazli,[a] Robert Tampé,[a] Bo Liedberg,[c] and Jacob Piehler*[a]

The dissection and functional characterization of cellular protein–protein interaction networks and multiprotein complexes will be a major challenge for life-science research in the coming years. To tackle the enormous number of potential interactions, new techniques are needed that are based on automated, highly multiplexed binding assays.[1–4] Here, approaches that combine label-free detection methods and protein-array formats are very promising,[5,6] and several label-free optical techniques have already been developed for parallel screening of protein interactions.[7–11] An often underestimated key problem, however, is immobilizing proteins into arrays, while maintaining their function. Affinity tags, which are recognized with high specificity by antibodies or other proteins, have frequently been employed for site-specific capturing of recombinant proteins. However, only a few of these traditional interaction pairs are suitable for protein immobilization, and the possibilities for multiplexed immobilization by differential recognition is therefore rather limited. Furthermore, protein-based recognition elements are not very compatible with microfabrication processes. In recent years, multivalent interaction has emerged as a powerful principle for engineering molecular recognition that provides the possibility of systematically tailor-binding affinities.[12–16] We have employed this approach for designing multivalent chelators (MCH) as high-affinity adapters for oligohistidine-tagged proteins.[17] We showed that the multivalency of the MCH as well as the redundancy (i.e. the number of excess binding sites) of the histidine-tag can be used to adjust the binding affinity in solution over several orders of magnitude. Furthermore, we have observed that redundancy modulates affinity even more strongly on surfaces[18] where the density of functional groups on that surface comes into play. This is a general, interesting feature of degenerate multivalent interactions due to the possibility of involving more than one recognition unit on the surface if the density is high enough (Figure 1 A).[19–21] This effect is termed "surface multivalency" in the following. Yet another interesting feature of multivalent complexes is the possibility of increasing the dissociation kinetics by addition of a competing, monovalent ligand at high concentration.[12] MCH/oligohistidine complexes can be readily dissociated by chasing with imidazole in a concentration-dependent manner. Thus, the dissociation kinetics of a histidine-tag at given imidazole concentrations depend on the molecular multivalency as well as the density of binding sites on the surface.[18,22]

Here, we present an approach towards differential immobilization and arraying of histidine-tagged proteins by combining molecular and surface multivalency. We employed recently described self-assembled monolayers (SAMs) formed by tri-ethylene glycol-terminated alkyl thiols functionalized with either a single nitrilotriacetic acid (NTA) moiety (mono-NTA) or with a novel chelator head group containing two NTA moieties (bis-NTA, Figure 1 B). The surface concentration of chelating thiols is adjusted by mixing these thiols with a matrix thiol carrying no NTA moiety. These mixed SAMs were shown to be biocompatible and suitable for precisely controlled immobilization of functional proteins.[22] Mono- and bis-NTA SAMs were assembled into microarrays by dispensing thiol solutions into a hydrophobic grid obtained by microcontact printing (μCP) of eicosanethiol (Figure 1 C).[23] By these means, we generated microarrays consisting of elements with different surface concentrations of chelator thiols as well as different types of chelators (mono- or bis-NTA). Increasing SAM thicknesses with increasing concentration of chelator thiol in solution were confirmed by imaging surface plasmon resonance (SPR, Figure 1 D). A detailed analysis of the SAMs by imaging ellipsometry confirmed a good correlation between surface and solution concentrations of the chelators.[23]

Immobilization of proteins, specific interaction with a ligand and elution with imidazole was monitored in a laterally resolved manner and in real time by imaging SPR in order to characterize the interaction between the surface and histidine-tagged proteins in different array elements. The extracellular domain of the type I interferon receptor subunit ifnar2 fused to a C-terminal hexa-(ifnar2-H6) or decahistidine-tag (ifnar2-H10) was immobilized on these surfaces (Figure 2 A). Typical binding curves recorded simultaneously for different elements of a bis-NTA density array are shown in Figure 2 A: immobilization of ifnar2-H10 (I) is followed by specific interaction with the ligand IFNα2 (II). Upon injection of 70 mM imidazole, the immobilized proteins are partially eluted (III), while a pulse of 400 mM imidazole completely regenerates the surface (IV). During elution with 70 mM imidazole, a strong dependence of the dissociation kinetics on the surface concentration of bis-NTA was observed; the lower the bis-NTA density, the faster the protein dissociated from the surface. Thus, the relative amount of protein remaining on the surface after this step increased with increasing chelator surface concentration (Figure 2 B). This result confirms that not only molecular multivalency, but also substantial surface multivalency is involved in the attachment of the histidine-tag to the chelator surface, thus leading to a more stable attachment of the protein at higher chelator density. For the highest surface concentration

[a] A. Tinazli, Prof. Dr. R. Tampé, Dr. J. Piehler
Goethe University Frankfurt/Main, Institute of Biochemistry
Max-von-Laue-Strasse 9, 60438 Frankfurt/Main (Germany)
Fax: (+49) 69-79829495

[b] Dr. R. Valiokas
Molecular Compounds Physics Laboratory, Institute of Physics
Savanoriu 231, 02300 Vilnius (Lithuania)

[c] G. Klenkar, Prof. Dr. B. Liedberg
Division of Molecular Physics
Department of Physics, Chemistry and Biology, Linköping University
581 83 Linköping (Sweden)

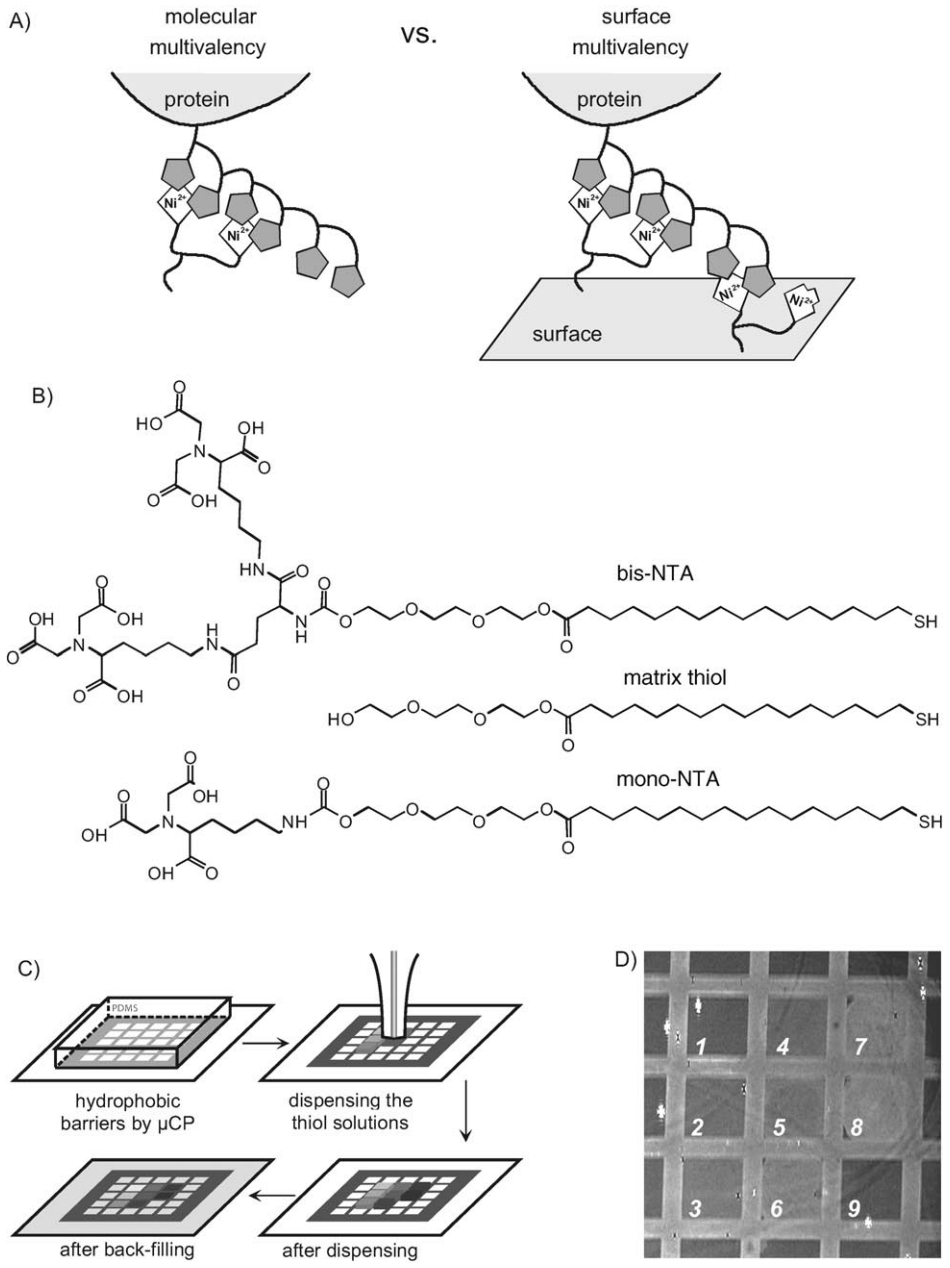

Figure 1. Tailored molecular and surface multivalency. A) Schematic recognition of a hexahistidine-tagged protein by a bis-NTA head group (left) and by two bis-NTA moieties tethered to a surface (right). B) Chemical structures of the chelator and matrix thiols. C) Fabrication of bis-NTA group density microarray by piezo-dispensing of chelator thiol mixtures into a hydrophobic grid obtained by μCP of eicosanethiol . After the density array had been dispensed, the remaining array elements were back-filled by immersing the array in matrix thiol, and excess chelator thiols were removed. D) Typical bis-NTA density array as visualized by imaging SPR—1: 0 mol% (dispensed); 2: 1 mol%; 3: 2 mol%; 4: 5 mol%; 5: 10 mol%; 6: 20 mol%; 7: 30 mol%; 8: 50 mol%; 9: 0 mol% (back-filled).

(50 mol% bis-NTA) less than 20% of the protein was eluted, whereas more than 90% was eluted for the lowest surface concentration (1 mol% bis-NTA, Figure 2B). Similar experiments were carried out with mono-NTA, and elution of ifnar2-H6 was also studied (data not shown). Differences in the binding affinity of bis-NTA and mono-NTA surfaces were found to be somewhat stronger for ifnar2-H6 than for ifnar2-H10.

Based on these screens, mono-NTA and bis-NTA density arrays were fabricated on the same chip. A comparison of the elution of ifnar2-H6 from an array with two different concentrations of mono-NTA and bis-NTA simultaneously monitored by imaging SPR is shown in Figure 2C. Strikingly, very different dissociation kinetics were observed for mono-NTA and bis-NTA, with the most profound difference at a concentration of 15 mol%. The strong stabilization by molecular multivalency of bis-NTA was confirmed even at high chelator concentrations; the protein dissociated much faster at 30 mol% mono-NTA than at 15 mol% bis-NTA, despite the same effective surface concentrations of NTA head groups. The effect of the differential elution is demonstrated by the SPR images recorded during the course of a typical experiment on a 2×2 array of mono- and bis-NTA at concentrations of 5 mol% and 15 mol% (Figure 2D). After immobilization of ifnar2-H6, the protein was eluted with 40 mM imidazole, and ifnar2-H6 was then reloaded. These images demonstrate the homogeneous behavior within each array element in terms of protein-loading capacity as well as the level of protein remaining on the surface upon elution with imidazole. Furthermore, the images demonstrate the much higher stability of ifnar2-H6 attached to bis-NTA compared to mono-NTA. However, the eluted protein was restored to close to the original levels during a second injection of ifnar2-H6.

A detailed experiment assessing protein immobilization and the differential elution and functionality of the immobilized proteins is shown in Figure 3A for the array elements with 15% mono-NTA and 15% bis-NTA. After the surface had been loaded with Ni^{II} ions (not shown), similar levels of stably immobilized ifnar2-H6 were obtained on both array elements (I). Injection of 40 mM imidazole, however, resulted in nearly exclusive elution from the mono-NTA array element (II). The activity of the immobilized protein was then probed by injecting 2 μM of the ligand IFNα2M148A, which binds to ifnar2-EC with an equilibrium dissociation constant of

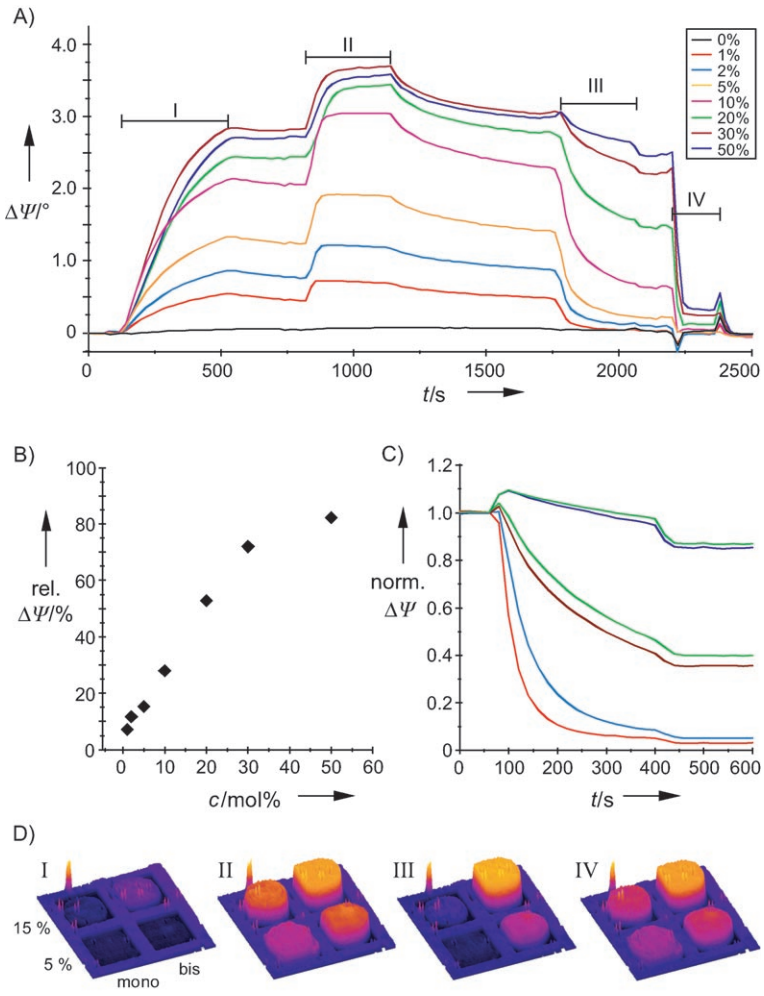

Figure 2. Immobilization and differential elution on a bis-NTA density array. A) Binding assay on the bis-NTA density array shown in Figure 1C. I) immobilization of ifnar2-H10, II) binding of the ligand IFNα2, elution with III) 70 mM and IV) 400 mM imidazole. B) Relative amount of protein remaining on the surface after elution with 70 mM imidazole (step III) at different densities of bis-NTA. C) Elution of ifnar2-H6 from mono-NTA (bright colors) and bis-NTA (dark colors) density arrays in comparison (red: 5 mol%; blue: 15 mol%; green: 30 mol%). D) SPR images of a comparative protein-binding experiment with 5 and 15 mol% mono- and bis-NTA. I) after conditioning by treatment with 10 mM Ni^{II} ions and 200 mM imidazole, II) after immobilization of ifnar2-H6, III) after elution with 40 mM imidazole, IV) after reloading ifnar2-H6.

~200 nM.[24] The binding signal confirmed nearly complete elution of ifnar2-H6 (III), yet the residual protein was still fully active in terms of ligand binding. During subsequent injection of ifnar2-H6, strong binding was observed to the mono-NTA array element, but not to the bis-NTA array element (IV). Injection of the ligand after reloading ifnar2-H6 gave very similar binding signal on both channels (V). All proteins could be removed from the surface by injection of imidazole at high concentration (VI). Upon injection of 40 mM imidazole, nearly 90% of the protein was removed from the mono-NTA array element, in contrast to only ~10% on the bis-NTA array element. After reloading, ~80% of the initial loading was achieved for mono-NTA, while bis-NTA reached the same level as before elution. Probably loss of Ni^{II} ions during elution is responsible for the somewhat lower binding capacity after elution. The binding signals during injection of the ligand are compared in Figure 3D. Indeed, very similar levels were reached after refilling the mono-NTA array element.

In order to further demonstrate potential applications of the differential immobilization procedure in the field of protein chips, we carried out a proof-of-principle experiment with two different variants of ifnar2-EC immobilized into the same mono- and bis-NTA density array as used for the previous experiment. Again, ifnar2-H6 was loaded in the first step, but after elution with imidazole, ifnar2-H10 I47A was loaded (not shown), which binds IFNα2 with an approximately tenfold lower affinity.[25] Strikingly, differential dissociation kinetics were detected upon injection of wild-type IFNα2 (Figure 3E), in agreement with the binding curves obtained for wild-type and mutant ifnar2-EC separately (not shown). The small apparent difference in the dissociation kinetics was due to strong rebinding, because the flow system was not optimized for mass-transport.

Our results demonstrate that proteins can be selectively targeted into different array elements by engineering immobilization stability based on combined molecular and surface multivalency. The fabrication of the density arrays by piezo-dispensing thiol solutions in a controlled and reproducible manner proved particularly important for rapid optimization of the conditions for differential immobilization. Much more versatility could be incorporated by using different MCHs to further increase the molecular affinity,[17] by designing arrays with combined different MCHs on surfaces, and by engineering histidine-tags with different lengths, different binding motifs, and different spacer lengths. Next to multiplexed in situ immobilization of different proteins for parallel screening of drugs and ligands, the possibility of mixing proteins in different ratios opens exciting perspectives for studying multiprotein complexes or for optimizing multienzymatic reactions.

Experimental Section

The preparation and characterization of NTA thiol density arrays are described in more detail elsewhere.[23] Briefly, a hydrophobic grid was obtained by μCP by using a PDMS stamp with 125-μm-wide protruding frames separating a 10×10 array of 375-μm-wide recessed squares. The stamp was inked with eicosanethiol (0.2 mM) in ethanol for 30–60 s, dried with N_2 gas, and applied for 60 s onto freshly cleaned gold surfaces. Mixtures of mono- and bis-NTA thiols dissolved in ethanol were loaded into a 60-μm-diameter piezo-driven glass capillary (Microdrop GmbH, Norderstedt, Germany). The positions of the array elements were monitored by observing the condensation of water microdroplets on the surface cooled with a Peltier element. Successively and pairwise, a total of 14 drops were ejected from the dispenser onto the dry surface, at intervals of approximately 1–2 s. The chip was then incubated in

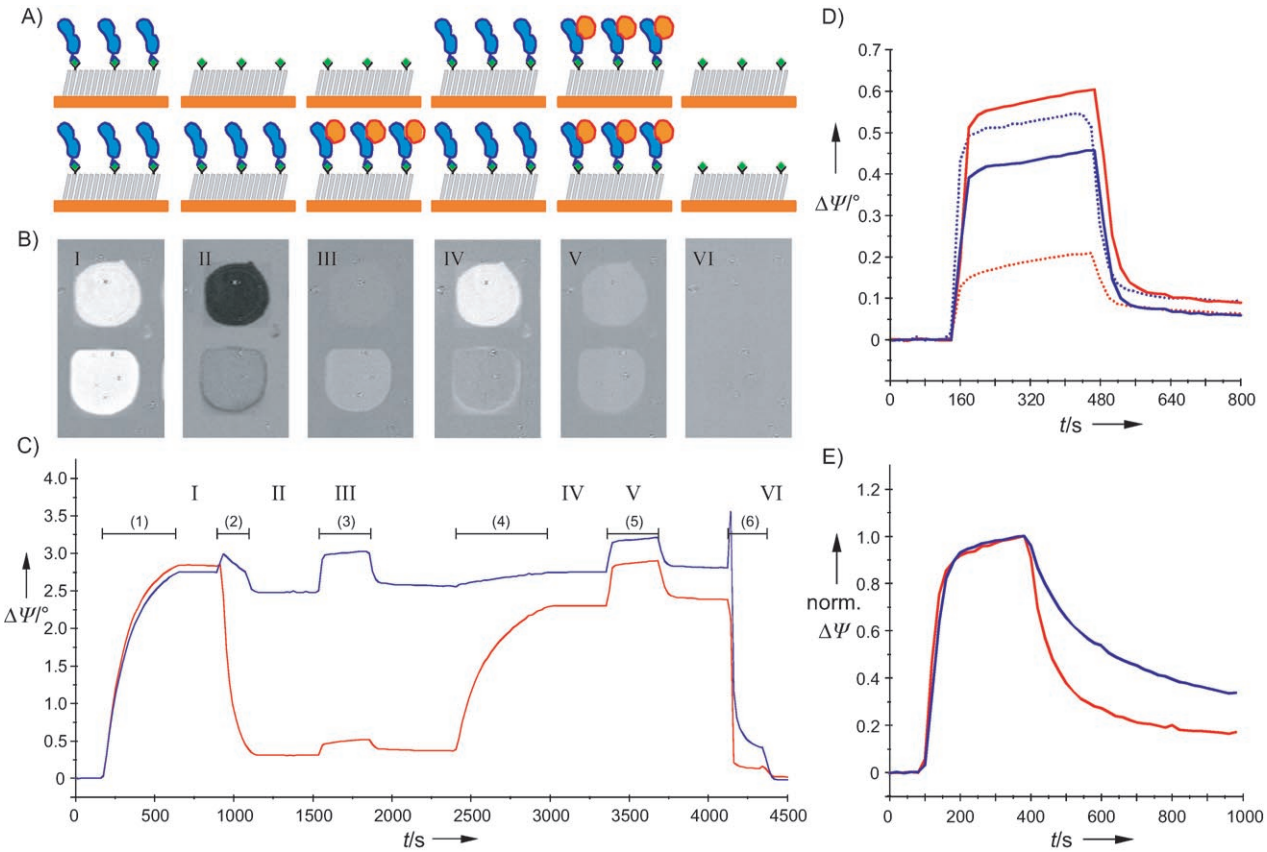

Figure 3. Differential elution of ifnar2-H6 from 15 mol% mono- and bis-NTA surfaces. A) Cartoon of the different states of the assay on the two array elements. I) immobilized ifnar2-H6, II) differential elution, III) ligand binding, IV) refilling of the eluted protein, V) ligand binding, and VI) regeneration. B) Difference images obtained by imaging SPR during the different steps of the assay (top: mono-NTA; bottom: bis-NTA; the brightness corresponds to the relative mass loading). Images II–V were obtained by subtracting the previous image, images I and VI were obtained by subtracting the image of the untreated chip. The Roman numerals refer to the respective time-points of taking the pictures as in indicated sensorgram (C). The sensorgram was corrected for background signal by subtracting the sensorgram from a reference array element (SAM without NTA groups). The injections are indicated with Arabic numerals: 1) 500 nM ifnar2-H6; 2) 40 mM imidazole; 3) 2 μM IFNα2M148A; 4) 500 nM ifnar2-H6; 5) 2 μM IFNα2M148A; 6) 400 mM imidazole. D) Ligand binding signals before (····) and after (——) reloading ifnar2-H10 (red: mono-NTA; blue: bis-NTA). E) Normalized binding curves of wild-type IFNα2 after differential elution from mono-NTA (red) and bis-NTA (blue) and selectively loading of ifnar2-H10 I47A onto the mono-NTA array element.

matrix thiol (1 mM in ethanol), followed by extensive rinsing in ethanol. Prior to binding assays, the chip was incubated in a solution of bovine serum albumin (1 mg mL^{-1}) in HEPES-buffered saline (HBS; 50 mM HEPES, pH 7.4, and 150 mM NaCl) in order to block nonspecific binding to the hydrophobic grid. Imaging SPR measurements were performed on an EP3 imaging null-ellipsometer (Nanofilm Technologie, Göttingen, Germany) equipped with a xenon lamp. The chip was mounted into a flow cell attached to a 60° SF 10 prism. Measurements were performed with a 2× magnification objective at a wavelength of 532 nm and an angle of incidence of 63.5°. SPR images were recorded as the reflectance of p-polarized light. Protein binding was monitored in real time by imaging SPR by using continuous flow injection analysis with a flow rate of 20 μL min^{-1}. The ellipsometric angle Ψ averaged over each region of interest was recorded over time at a sampling interval of 20 s. Sensorgrams were corrected for background signals by subtracting a sensorgram acquired at a reference array element (SAM without NTA groups). Sensorgrams are presented as the change of Ψ over time ($\Delta\Psi$). All measurements were carried out in HBS containing P20 (0.015% *w/w*). Proteins (300–500 nM in HBS) were immobilized onto chelator surfaces after loading the NTA head groups with Ni^{II} chloride (10 mM) in HBS.[22] After binding experiments, all proteins were removed with imidazole (200 mM) in HBS, and the NTA head groups were reloaded with Ni^{II} ions prior to the next immobilization cycle.

Acknowledgements

This work was supported by the DFG (research grants #Pi 405/1 and Pi 405/2 to J.P. and Ta 157/6 to R.T.) and by the BMBF (0312005A to J.P. and R.T.). The work was also supported by grants to B.L. from the Wallenberg Consortium North (WCN) and from the Foundation for Strategic Research (SSF) through the Biomimetic Materials Science Program. R.V. received support from the Lithuanian State Science and Studies Foundation and the Swedish Institute through the Visby program.

Keywords: arrays · multivalent interactions · nitrilotriacetic acid · protein–protein interactions · surface plasmon resonance

[1] G. MacBeath, S. L. Schreiber, *Science* **2000**, *289*, 1760.
[2] H. Zhu, M. Snyder, *Curr. Opin. Chem. Biol.* **2003**, *7*, 55.
[3] N. Ramachandran, E. Hainsworth, B. Bhullar, S. Eisenstein, B. Rosen, A. Y. Lau, J. C. Walter, J. LaBaer, *Science* **2004**, *305*, 86.

[4] P. Bertone, M. Snyder, *FEBS J.* **2005**, *272*, 5400.
[5] M. A. Cooper, *Anal. Bioanal. Chem.* **2003**, *377*, 834.
[6] H. J. Lee, Y. Yan, G. Marriott, R. M. Corn, *J. Physiol. (Oxford, UK)* **2005**, *563*, 61.
[7] O. Birkert, R. Tunnemann, G. Jung, G. Gauglitz, *Anal. Chem.* **2002**, *74*, 834.
[8] G. J. Wegner, A. W. Wark, H. J. Lee, E. Codner, T. Saeki, S. Fang, R. M. Corn, *Anal. Chem.* **2004**, *76*, 5677.
[9] K. Kroger, J. Bauer, B. Fleckenstein, J. Rademann, G. Jung, G. Gauglitz, *Biosens. Bioelectron.* **2002**, *17*, 937.
[10] B. T. Cunningham, P. Li, S. Schulz, B. Lin, C. Baird, J. Gerstenmaier, C. Genick, F. Wang, E. Fine, L. Laing, *J. Biomol. Screening* **2004**, *9*, 481.
[11] N. Ramachandran, D. N. Larson, P. R. Stark, E. Hainsworth, J. LaBaer, *FEBS J.* **2005**, *272*, 5412.
[12] J. Rao, J. Lahiri, L. Isaacs, R. M. Weis, G. M. Whitesides, *Science* **1998**, *280*, 708.
[13] M. Mammen, S. K. Choi, G. M. Whitesides, *Angew. Chem.* **1998**, *110*, 2908; *Angew. Chem. Int. Ed.* **1998**, *37*, 2755.
[14] P. I. Kitov, D. R. Bundle, *J. Am. Chem. Soc.* **2003**, *125*, 16271.
[15] A. Mulder, T. Auletta, A. Sartori, S. Del Ciotto, A. Casnati, R. Ungaro, J. Huskens, D. N. Reinhoudt, *J. Am. Chem. Soc.* **2004**, *126*, 6627.
[16] M. Mourez, R. S. Kane, J. Mogridge, S. Metallo, P. Deschatelets, B. R. Sellman, G. M. Whitesides, R. J. Collier, *Nat. Biotechnol.* **2001**, *19*, 958.
[17] S. Lata, A. Reichel, R. Brock, R. Tampé, J. Piehler, *J. Am. Chem. Soc.* **2005**, *127*, 10205.
[18] S. Lata, J. Piehler, *Anal. Chem.* **2005**, *77*, 1096.
[19] J. Rao, L. Yan, J. Lahiri, G. M. Whitesides, R. M. Weis, H. S. Warren, *Chem. Biol.* **1999**, *6*, 353.
[20] J. Huskens, A. Mulder, T. Auletta, C. A. Nijhuis, M. J. Ludden, D. N. Reinhoudt, *J. Am. Chem. Soc.* **2004**, *126*, 6784.
[21] A. Mulder, J. Huskens, D. N. Reinhoudt, *Org. Biomol. Chem.* **2004**, *2*, 3409.
[22] A. Tinazli, J. Tang, R. Valiokas, S. Picuric, S. Lata, J. Piehler, B. Liedberg, R. Tampé, *Chem. Eur. J.* **2005**, *11*, 5249.
[23] G. Klenkar, R. Valiokas, I. Lundström, A. Tinazli, R. Tampé, J. Piehler, B. Liedberg, *Anal. Chem.* **2006**, *78*, 3643.
[24] J. Piehler, L. C. Roisman, G. Schreiber, *J. Biol. Chem.* **2000**, *275*, 40425.
[25] J. Piehler, G. Schreiber, *J. Mol. Biol.* **1999**, *294*, 223.

Received: April 28, 2006
Published online on August 3, 2006

